nature nanotechnology

LETTERS

https://doi.org/10.1038/s41565-020-00800-4

Check for updates

Scalable and hierarchically designed polymer film as a selective thermal emitter for high-performance all-day radiative cooling

Duo Li[1,5], Xin Liu[1,5], Wei Li[2,3,5], Zhenhui Lin[1], Bin Zhu[1]✉, Zizhong Li[1], Jinlei Li[1], Bo Li[1], Shanhui Fan[2], Jiwei Xie[4] and Jia Zhu[1]✉

Traditional cooling systems consume tremendous amounts of energy and thus aggravate the greenhouse effect[1,2]. Passive radiative cooling, dissipating an object's heat through an atmospheric transparency window (8–13 μm) to outer space without any energy consumption, has attracted much attention[3–9]. The unique feature of radiative cooling lies in the high emissivity in the atmospheric transparency window through which heat can be dissipated to the universe. Therefore, for achieving high cooling performance, the design and fabrication of selective emitters, with emission strongly dominant in the transparency window, is of essential importance, as such spectral selection suppresses parasitic absorption from the surrounding thermal radiation. Recently, various materials and structures with tailored spectrum responses have been investigated to achieve the effect of daytime radiative cooling[6–8,10–15]. However, most of the radiative cooling materials reported possess broad-band absorption/emission covering the whole mid-infrared wavelength[11–15]. Here we demonstrate that a hierarchically designed polymer nanofibre-based film, produced by a scalable electrostatic spinning process, enables selective mid-infrared emission, effective sunlight reflection and therefore excellent all-day radiative cooling performance. Specifically, the C–O–C (1,260–1,110 cm^{-1}) and C–OH (1,239–1,030 cm^{-1}) bonding endows the selective emissivity of 78% in 8–13 μm wavelength range, and the design of nanofibres with a controlled diameter allows for a high reflectivity of 96.3% in 0.3–2.5 μm wavelength range. As a result, we observe ~3 °C cooling improvement of this selective thermal emitter as compared to that of a non-selective emitter at night, and 5 °C sub-ambient cooling under sunlight. The impact of this hierarchically designed selective thermal emitter on alleviating global warming and temperature regulating an Earth-like planet is also analysed, with a significant advantage demonstrated. With its excellent cooling performance and a scalable process, this hierarchically designed selective thermal emitter opens a new pathway towards large-scale applications of all-day radiative cooling materials.

Compared with a selective thermal emitter, a non-selective thermal emitter with absorption/emission beyond the atmospheric transparency window will absorb downward thermal radiation from the atmosphere and therefore compromise the cooling performance (Fig. 1a). Theoretical calculation shows that the ideal selective emitter allows for a larger temperature drop than that of the non-selective emitter (Fig. 1b,c)[6]. Such a selective emissivity spectrum has been previously demonstrated using a near-ideal selective emitter based on a one-dimensional photonic crystal[7,10]. However, this photonic crystal emitter, fabricated by photolithography and electron beam evaporation, has limited scalability.

As emission in the mid-infrared region is typically associated with molecular bonding, molecular-level design with appropriate chemical bonding provides a more convenient and scalable pathway, compared to complex top-down fabrication, to enable narrow band and selective absorption/emission in the mid-infrared region for radiative cooling.

It is revealed that vibrational absorptions in the mid-infrared waveband outside the atmospheric window (8–13 μm) are usually caused by various bond vibrations, including –CHO (2,810–2,710 cm^{-1}), C=C (1,880–1,785 cm^{-1}), C=O (1,825–1,725 cm^{-1}) and C–S (weak vibrational peaks at 600–650 cm^{-1}), as well as S–S bond vibrations (below 500 cm^{-1}). These bonds should be excluded for constructing a selective thermal emitter. By contrast, polymers that have bonds vibrating only at 8–13 μm, such as C–O–C (1,260–1,110 cm^{-1}), C–OH (1,239–1,030 cm^{-1}), $-CF_3$ (1,148 cm^{-1}) and Si–O–Si (1,100 cm^{-1}), have great potential as an ideal selective thermal emitter. Therefore, among all the polymer films, it is expected that polyethylene oxide (PEO), which has only C–C, C–O and C–H bonds, presents a desirable selective absorption band, overlapping with the atmospheric transparency window (8–13 μm; Fig. 1d).

Besides selective thermal emission in the atmospheric transparency window (8–13 μm), strong reflection of the solar spectrum (0.3–2.5 μm) is also necessary to realize high-performance all-day radiative cooling. However, a typical PEO film fabricated through drop-casting is visibly transparent (Supplementary Fig. 1), which cannot meet the demand for high sunlight reflectance. Nanofibres with diameters comparable to the wavelength of the solar spectrum can serve as effective scatterers to enable strong solar reflection (Fig. 1e).

Combining the designs at the molecular level and nanoscale mentioned above, we synthesize PEO films composed of random nanofibres as daytime radiative coolers through a scalable roll-to-roll electrospinning method (Fig. 1f and Supplementary Video). Specifically, this hierarchically designed PEO film demonstrates desirable properties for radiative cooling, with an average selective emittance of 78% in the wavelength range of 8–13 μm and a high reflectance of 96.3% in the sunlight region (0.3–2.5 μm).

[1]National Laboratory of Solid State Microstructures, College of Engineering and Applied Sciences, Jiangsu Key Laboratory of Artificial Functional Materials and Collaborative Innovation Center of Advanced Microstructures, Nanjing University, Nanjing, P. R. China. [2]Ginzton Laboratory, Department of Electrical Engineering, Stanford University, Stanford, California, USA. [3]State Key Laboratory of Applied Optics, Changchun Institute of Optics, Fine Mechanics and Physics, Chinese Academy of Sciences, Changchun, China. [4]School of Astronomy and Space Science, Nanjing University, Nanjing, P. R. China. [5]These authors contributed equally: Duo Li, Xin Liu, Wei Li. ✉e-mail: binzhu@nju.edu.cn; jiazhu@nju.edu.cn

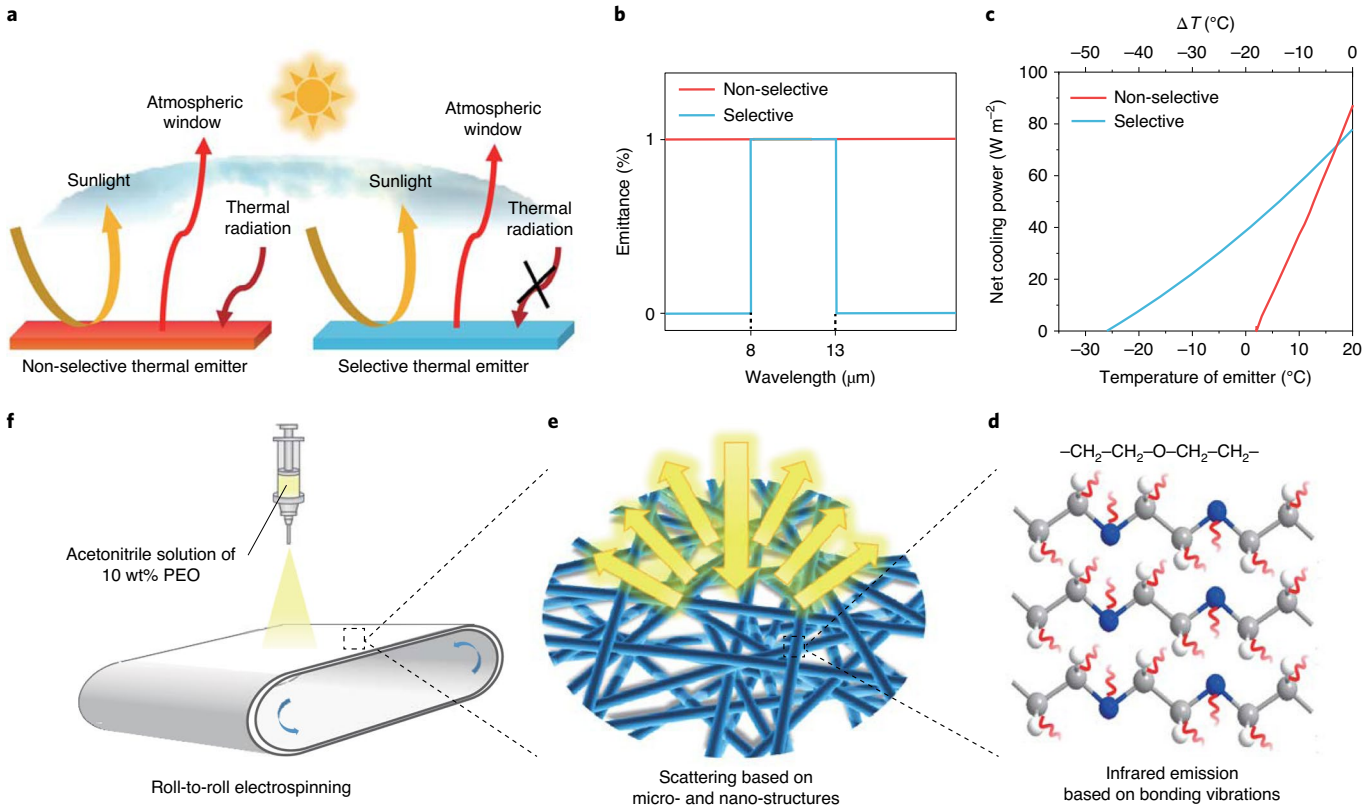

Fig. 1 | The theoretical analysis and fabrication process of the selective thermal emitter. a, The schematic of the radiative heat transfer process of a selective and a non-selective thermal emitter. Both the selective and non-selective thermal emitters highly reflect sunlight and emit strongly through the atmospheric window. The selective thermal emitter has a suppressed absorption of thermal radiation from the surroundings compared to that of the non-selective emitter. **b**, The mid-infrared spectrum of an ideal selective thermal emitter (blue line) and a non-selective thermal emitter (red line). **c**, Net cooling power as a function of the emitter temperature. The calculation is based on a typical atmospheric transmittance (blue line in Fig. 2g) and parasitic heat transfer coefficient $h = 0\ \mathrm{W\,m^{-2}\,K^{-1}}$. **d**, Schematic of infrared emission by bond vibrations of the PEO molecular chain. Grey ball, C atom; blue ball, O atom; white ball, H atom. **e**, Effective scattering of micro- and nano-structures of the es-PEO film. **f**, Schematic of the scalable fabrication process, roll-to-roll electrospinning.

As electrostatic spinning with significant advancement provides a scalable process to fabricate nanofibres[16–24], a modified roll-to-roll electrostatic spinning method is developed and applied to produce the hierarchically designed PEO film (Supplementary Fig. 2; details in Methods). Figure 2a shows a roll of electrostatic spinning PEO (es-PEO) film that was produced, which is several metres long, a quarter metre wide and 500 μm thick (Supplementary Fig. 3). Its white colour illustrates the strong scattering of visible light, which is ascribed to the multilayer structure of randomly stacked nanofibres with diameter sizes broadly distributed (centred at ~800 nm; Fig. 2b,c). As corroborated by the scattering efficiency calculation of the PEO nanofibre as a function of diameter size across the solar spectrum using Mie theory (Fig. 2d), the obtained nanofibre with the diameter distributed in the 500–1,200 nm range can strongly scatter the sunlight (especially in the 0.3–1.2 μm wavelength range, which covers most of the solar wavelength range). Another feature of PEO that is ideal for radiative cooling is that it has negligible material absorption loss over the entire solar wavelength range (Fig. 2e and Supplementary Fig. 4). The strong sunlight reflection by these multilayer random PEO nanofibres is confirmed by the calculations based on Mie theory together with Chandrasekhar radiative transfer theory (Fig. 2f). Figure 2g shows the optical spectrum of the es-PEO film, with a high reflectivity of more than 96.3% in the sunlight region, high emissivity of 78% in the wavelength region 8–13 μm and low emissivity outside the atmospheric transparency window, ideal for all-day radiative cooling.

To experimentally verify the radiative cooling performance of the hierarchically designed es-PEO film, we performed a continuous outdoor measurement of the temperature and cooling power on a clear day at Nanjing. As shown in Fig. 3a,b, the device consists of an acrylic shell covered with a layer of Al foil to reflect the radiation from the surrounding buildings, a foam insulation sample stage, a heater and a layer of infrared-transparent wind cover polyethylene (PE) film (Supplementary Fig. 5), consistent with previous studies[25]. In the daytime, the es-PEO film shows a sub-ambient temperature drop of $|\Delta T| \approx 5\,^{\circ}\mathrm{C}$ even under the peak solar intensity of near $900\ \mathrm{W\,m^{-2}}$ at noon (Fig. 3c and Supplementary Fig. 6). The corresponding cooling power of the es-PEO film reaches as high as $110\ \mathrm{W\,m^{-2}}$ (Fig. 3d). This experiment confirms that the obtained es-PEO film stands out as a high-performance radiative cooling material during the daytime.

To further evaluate the cooling difference of the es-PEO film as a result of selective thermal emission, we chose a dyed-black fabric with non-selective thermal emission in the mid-infrared region for comparison (Fig. 3e). The tests were carried out at night to exclude the effect of sunlight. It is obvious that the es-PEO film is consistently ~3 °C cooler compared to the dyed-black fabric sample throughout the test (Fig. 3f and Supplementary Fig. 7), and ~7 °C below ambient temperature. All the results consistently suggest that the prepared es-PEO film has an excellent cooling performance as a result of selective thermal emission. For future real-world applications, durability is an important parameter of radiative cooling materials. Chemical

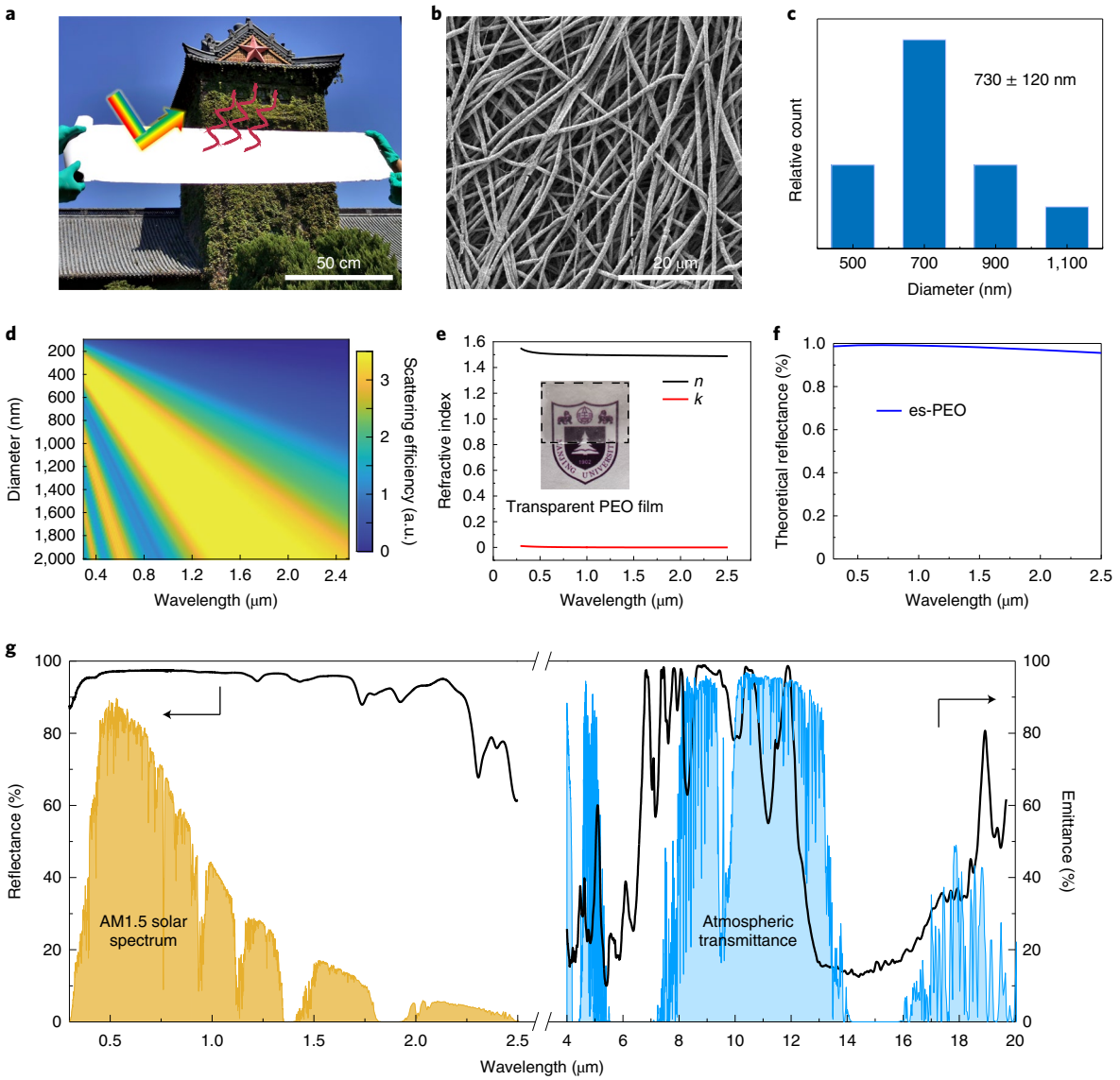

Fig. 2 | The structures and optical properties of es-PEO. a, A photo of an es-PEO thin film produced by roll-to-roll electrospinning. The thickness of the film is 500 μm. **b**, Scanning electron microscopy images of random nanofibres of the es-PEO thin film. **c**, The statistical distribution of the diameters of the PEO fibres demonstrated in **b**. **d**, Simulation of the scattering efficiency of PEO nanofibres over the wavelength range of 0.3–2.5 μm with the fibre diameter varied from 100 to 2,000 nm. a.u., arbitrary units. **e**, The complex spectral refractive index ($n+ik$) of PEO in the solar wavelength range. Inset: optical image of transparent PEO film fabricated through drop-casting method). **f**, Theoretical reflectance spectrum of es-PEO. **g**, Spectral UV–visible–infrared reflectance/emittance of a 500 μm es-PEO film (black line) presented against the AM1.5 solar spectra and the atmospheric transparency window.

cross-linking proves to be effective to improve the durability of our PEO-based selective thermal emitter (Supplementary Fig. 8).

It is expected that this es-PEO film with selective thermal emission is advantageous at a large scale. For example, the temperature of Earth is essentially balanced by absorbing radiation from the sun (6,000 K) and emitting thermal radiation to the cold outer space (3 K) simultaneously (Fig. 4a). As the unique feature of radiative cooling is that it can send the heat to space through an atmospheric transparency window (8–13 μm), radiative cooling is considered a technical solution to alleviate global warming[26–28]. The es-PEO film with selective infrared emittance and high scalability is particularly ideal for this purpose. By placing the radiative materials in a desert that is dry and hot (temperatures as high as ~323 K) and has a low population density, the potential energy savings and laying area size can be calculated. The es-PEO film with selective emittance is more effective compared to one with non-selective emittance (Supplementary Fig. 9). When the temperature drop is higher, the es-PEO selective emitter shows higher cooling power than that of the non-selective thermal emitter (Fig. 4b; $\Delta P = P_{\text{selective}} - P_{\text{non-selective}}$). For temperatures reaching 305 K, the data show that the surface area required when laying the es-PEO selective emitter is 1.17×10^7 km^2 (Fig. 4c), while that required with the non-selective emitter is 1.51×10^7 km^2 (~30% more); the difference is the equivalent of laying the material over the entire Gobi and Rub Al Khal deserts (Fig. 4d).

Earth-like planets, which typically possess rock, metals, water and a thin atmosphere, and have similar mass, size and temperature to Earth[29], are considered potential candidates for future space colonization. However, a higher temperature at their surface compared to the Earth (288 K) impedes the survival of life. As a typical example, the planet Kepler-62e, which is located in the Kepler-62 system and has a similar orbit and atmospheric composition as Earth[30], shows a much high surface temperature[31] (340 K; Fig. 4e).

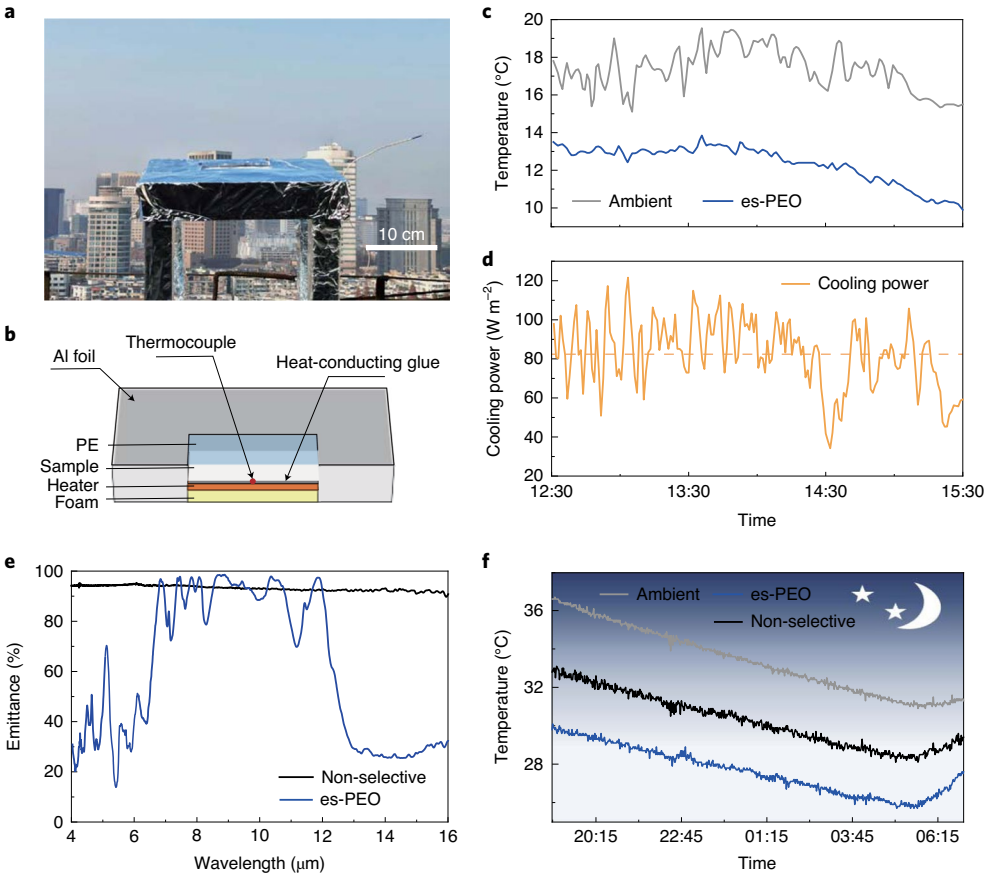

Fig. 3 | Cooling performance of a selective emitter es-PEO film, in comparison with a non-selective emitter. a, Set-up of the real-time measurement of the radiative cooling performance. **b**, Schematic of the set-up for testing the radiative cooling power and cooling temperature. **c**,**d**, Real-time temperature (**c**) and cooling power (**d**) data of the outdoor experiment with the es-PEO film in Nanjing (date, 11 December 2019, UTC+8). **e**, Mid-infrared emittance spectra of the measured es-PEO film and the control sample of a dyed-black fabric. **f**, Night-time temperatures of two cooling samples compared with ambient temperature (date, 14 September 2019, UTC+8).

According to modelling of the radiation intensity of Kepler-62 (ref. [32]; Supplementary Fig. 10), a thermal emitter can be used to regulate the surface temperature of Kepler-62e to a more habitable temperature range. The emission spectra of thermal emitters vary from non-selective to ideally selective (spectral tuning process shown in Supplementary Fig. 11). Figure 4f shows the theoretical cooling performance of thermal emitters with various emission spectra, in which the es-PEO film (mean) can cool Kepler-62e from 340 K to 295 K (the temperature reduction is 45 K) while the non-selective emitter (78%) has a temperature drop of only 33 K. This example once again illustrates that our hierarchically designed selective thermal emitter shows a better cooling performance compared with a non-selective thermal emitter. More importantly, the selective thermal emitter has great potential to cool the planet Kepler-62e to the ideal temperature of 288 K (the same temperature as Earth), and the emitter with a limited emission spectrum can even reach a cooling temperature limit of 244 K (Fig. 4f), showing great potential in making Earth-like planets habitable.

In conclusion, we demonstrate a hierarchically designed (molecular level and nanoscale), high-performance radiative cooling material with a strong selective emittance in the atmospheric transparency window. This PEO-nanofibre-based film is scalable and produced via a roll-to-roll electrospinning process. It shows a high reflectance in the sunlight region because of its disordered photonic structure with innumerable nanofibres, and a selective emittance in the mid-infrared region due to its specific bond vibrations. Both real-time temperature measurements and theoretical calculations confirm the superior cooling performance of the PEO film compared to a non-selective thermal emitter. This selective thermal emitter provides a more viable pathway for alleviating the global warming of the Earth and for temperature regulating an Earth-like planet. It provides new routes for developing large-scale and high-performing radiative cooling technologies towards an energy-efficient and sustainable society. In addition, it can inspire more molecular/chemical designs and an interdisciplinary effort for advanced photonic materials and devices.

Online content

Any methods, additional references, Nature Research reporting summaries, source data, extended data, supplementary information, acknowledgements, peer review information; details of author contributions and competing interests; and statements of data and code availability are available at https://doi.org/10.1038/s41565-020-00800-4.

Received: 5 June 2020; Accepted: 19 October 2020;
Published online: 16 November 2020

References

1. Walther, G. R. et al. Ecological responses to recent climate change. *Nature* **416**, 389–395 (2002).

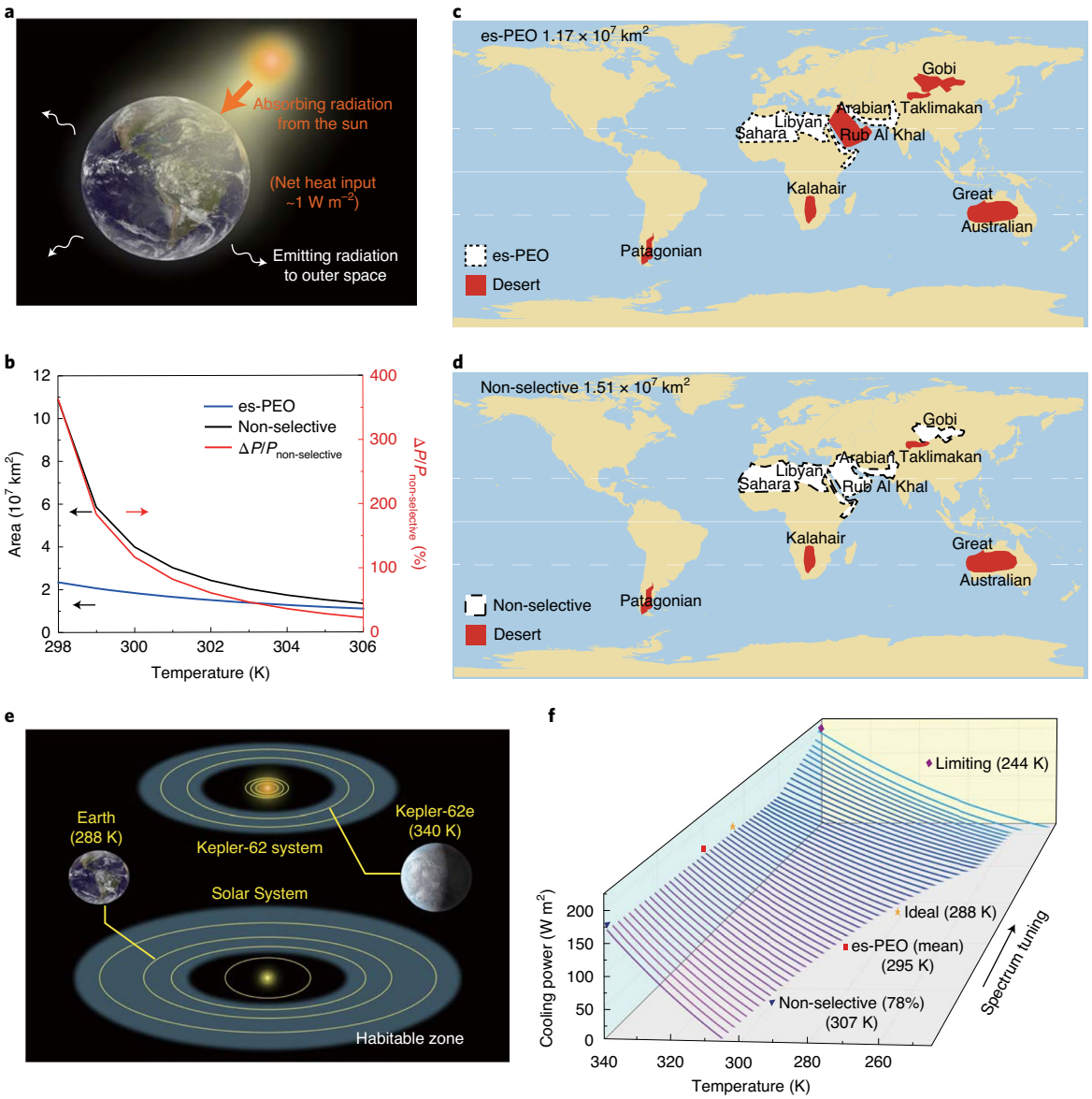

Fig. 4 | The simulation of cooling Earth and the high-temperature Earth-like planet Kepler-62e. a, The radiation absorbed from the Sun heats the Earth, while the radiation emitted to outer space causes cooling. The ~1 W m^{-2} net heat input warms the Earth. **b**, The needed area of es-PEO and non-selective thermal emitter to offset 1 W m^{-2} heat input, and the cooling savings of es-PEO compared with a non-selective thermal emitter. **c**,**d**, Schematics of using es-PEO (**c**) and non-selective thermal emitter (**d**) globally. The red shading is the area of the top ten deserts by size of the world, while the white areas within the black dashed lines are the areas used for radiative cooling. **e**, Schematic of the Kepler-62 system and Solar System. The horizontal lines from top to bottom are the tropic of Cancer, the equator and the tropic of Capricorn. **f**, Net cooling power as a function of the thermal-emitter temperature with various emission spectra. Credit: © NASA (**a**,**e**) and Esri (**c**,**d**).

2. Cook, B. I., Smerdon, J. E., Seager, R. & Coats, S. Global warming and 21st century drying. *Clim. Dyn.* **43**, 2607–2627 (2014).
3. Catalanotti, S. et al. The radiative cooling of selective surfaces. *Sol. Energy* **17**, 83–89 (1975).
4. Granqvist, C. G. & Hjortsberg, A. Radiative cooling to low temperatures: general considerations and application to selectively emitting SiO films. *J. Appl. Phys.* **52**, 4205–4220 (1981).
5. Gentle, A. & Smith, G. Radiative heat pumping from the earth using surface phonon resonant nanoparticles. *Nano Lett.* **10**, 373–379 (2010).
6. Rephaeli, E., Raman, A. & Fan, S. Ultrabroadband photonic structures to achieve high-performance daytime radiative cooling. *Nano Lett.* **13**, 1457–1461 (2013).
7. Raman, A. P., Anoma, M. A., Zhu, L., Rephaeli, E. & Fan, S. Passive radiative cooling below ambient air temperature under direct sunlight. *Nature* **515**, 540–544 (2014).
8. Zhao, D. et al. Radiative sky cooling: fundamental principles, materials, and applications. *Appl. Phys. Rev.* **6**, 021306 (2019).
9. Li, W. & Fan, S. Radiative cooling: harvesting the coldness of the universe. *Opt. Photon. News* **30**, 32–39 (2019).
10. Chen, Z., Zhu, L., Raman, A. & Fan, S. Radiative cooling to deep sub-freezing temperatures through a 24-h day–night cycle. *Nat. Commun.* **7**, 13729 (2016).
11. Goldstein, E. A., Raman, A. & Fan, S. Sub-ambient non-evaporative fluid cooling with the sky. *Nat. Energy* **2**, 17143 (2017).
12. Zhai, Y. et al. Scalable-manufactured randomized glass-polymer hybrid metamaterial for daytime radiative cooling. *Science* **355**, 1062–1066 (2017).
13. Li, T. et al. A radiative cooling structural material. *Science* **364**, 760–763 (2019).
14. Mandal, J. et al. Hierarchically porous polymer coatings for highly efficient passive daytime radiative cooling. *Science* **362**, 315–318 (2018).
15. Zhou, L. et al. A polydimethylsiloxane-coated metal structure for all-day radiative cooling. *Nat. Sustain.* **2**, 718–724 (2019).

16. Drury, J. L. & Mooney, D. J. Hydrogels for tissue engineering: scaffold design variables and applications. *Biomaterials* **24**, 4337–4351 (2003).
17. Wang, H. et al. Graphene-wrapped sulfur particles as a rechargeable lithium–sulfur battery cathode material with high capacity and cycling stability. *Nano Lett.* **11**, 2644–2647 (2011).
18. Liu, T. et al. Drug delivery with PEGylated MoS_2 nano-sheets for combined photothermal and chemotherapy of cancer. *Adv. Mater.* **26**, 3433–3440 (2014).
19. Li, D., Babel, A., Jenekhe, S. A. & Xia, Y. Nanofibers of conjugated polymers prepared by electrospinning with a two-capillary spinneret. *Adv. Mater.* **16**, 2062–2066 (2004).
20. Yang, D., Lu, B., Zhao, Y. & Jiang, X. Fabrication of aligned fibrous arrays by magnetic electrospinning. *Adv. Mater.* **19**, 3702–3706 (2007).
21. Hu, X. et al. Electrospinning of polymeric nanofibers for drug delivery applications. *J. Control. Release* **185**, 12–21 (2014).
22. Liu, M. et al. A review: electrospun nanofiber materials for lithium–sulfur batteries. *Adv. Funct. Mater.* **29**, 1905467 (2019).
23. Wang, Y., Wang, S. & Lou, X. W. Dispersed nickel cobalt oxyphosphide nanoparticles confined in multichannel hollow carbon fibers for photocatalytic CO_2 reduction. *Angew. Chem. Int. Ed.* **58**, 17236–17240 (2019).
24. Han, K. S. et al. Electrically activated ultrathin PVDF-TrFE air filter for high-efficiency $PM_{1.0}$ filtration. *Adv. Funct. Mater.* **29**, 1903633 (2019).
25. Zhao, D. et al. Subambient cooling of water: toward real-world applications of daytime radiative cooling. *Joule* **3**, 111–123 (2019).
26. Manney, G. L. et al. Unprecedented Arctic ozone loss in 2011. *Nature* **478**, 469–475 (2011).
27. Munday, J. N. Tackling climate change through radiative cooling. *Joule* **3**, 2057–2060 (2019).
28. Stephens, G. L. et al. An update on Earth's energy balance in light of the latest global observations. *Nat. Geosci.* **5**, 691–696 (2012).
29. Seager, S. The search for extrasolar Earth-like planets. *Earth Planet. Sci. Lett.* **208**, 113–124 (2003).
30. Kaltenegger, L., Sasselov, D. & Rugheimer, S. Water-planets in the habitable zone: atmospheric chemistry, observable features, and the case of Kepler-62e and -62f. *Astrophys. J. Lett.* **775**, 1384–1395 (2013).
31. VPL Spectral Explorer. *NASA Astrobiology Institute Virtual Planetary Laboratory* http://depts.washington.edu/naivpl/content/vpl-spectral-explorer (2012).
32. Vladilo, G., Silva, L., Murante, G., Filippi, L. & Provenzale, A. Modeling the surface temperature of Earth-like planets. *Astrophys. J. Lett.* **804**, 50 (2015).

Methods

Fabrication of es-PEO film. First, the solution of 10 wt% PEO was obtained by intermittently adding PEO powder to acetonitrile. The mixture of PEO and acetonitrile was stirred. The resulting PEO solution was electrospun at a voltage of 18 kV, a spinning distance of 18 cm, a feeding rate of 4 ml h^{-1} and using a 20-gauge needle tip. The collector of the electrospun nanofibres consisted of a couple of rotation drums, a belt and a lap of nonwoven fabric, and the rotation speed was 100 r.p.m. The production rate can be enhanced for an industry-scale process, and we anticipate that the yield of es-PEO film can reach as high as 600 m^2 per day using electrospinning with wire electrodes.

Cross-linking of PEO and polypropylene glycol (PPG). First, a mixed solution of 10 wt% PEO and PPG was obtained by adding PEO and PPG sequentially to acetonitrile. The mass ratio of PEO and PPG was 1:1. The mixture of PEO, PPG and acetonitrile was stirred at 110 °C. After stirring evenly and cooling to room temperature, dicumyl peroxide was added as a cross-linking agent to the mixed solution. Afterwards, the resulting mixed solution was used to electrospin the film at a voltage of 18 kV. UV light was applied to the obtained PEO–PPG film under the protection of nitrogen for 30 min.

Optical characterization of es-PEO film. The spectroscopic performance of the es-PEO film was characterized separately in the UV to near-infrared (0.3–2.5 μm) and mid-infrared (2.5–20 μm) wavelength ranges. In the first range, the optical reflectance spectrum was measured using an UV–visible–near-infrared spectrophotometer (UV 3600, Shimadzu) equipped with an integrating sphere model (ISR-3100). For the second range, a Fourier transform infrared spectrometer (Nicolet IS50, ThermoFisher) and a gold integrating sphere (IntergatIR MIR, Pike) along with a mercury cadmium telluride (MCT-B) detector and KBr beam splitter were used together to measure the absorption spectra. Transmission spectra (0.3–2.5 μm) were obtained by the UV–visible–near-infrared spectrophotometer (UV 3600, Shimadzu) equipped with an integrating sphere model (ISR-3100), with the PEO cooling film placed at the mouth of the integrating sphere.

Microscopy measurement. The surface morphology of the es-PEO cooling film was characterized by a scanning electron microscope (TESCAN MIRA3).

Refractive index measurements. Refractive index measurements of PEO films were taken by an RC2 XI+.

Outdoor radiative cooling performance measurements. We tested the real-time temperature and cooling power using two set-ups simultaneously on the roof of a building at Nanjing University (32° 3′ 18.8″ N, 118° 46′ 33.2″ E). In each set-up, a piece of cooling sample with a size of 17.5 cm × 9.4 cm was used. The cooling power test set-up had a heater with a feedback control system to maintain ambient temperature. The two test set-ups were placed on a platform at a height of 1 m over the ground. A moisture recorder was placed beside the set-up to record the moisture during the test period.

Theoretical thermal calculation of the emitter. We used a simple model to analyse the energy balance of the thermal emitter, with several parts to the radiation: the emitted thermal radiation from the thermal emitter (P_{rad}), the absorbed thermal radiation from the atmosphere (P_{atm}), the heat transfer by thermal conduction and thermal convention ($P_{cond+conv}$) and the absorbed thermal radiation from sunlight (P_{solar}; $P_{solar}=0$ during night-time). The energy balance equation is as follows:

$$P_{net-cooling} = P_{rad} - P_{atm} - P_{solar} - P_{cond+conv}$$

The temperature reduction of the thermal radiation reached a steady state when the net cooling power $P_{net\text{-}cooling}=0$. The steady-state temperature of the selective thermal emitter is much lower than that of the non-selective thermal emitter.

Data availability

All relevant data are included in the manuscript and Supplementary Information. More detailed protocols, calculations and analysis are available from the authors upon request.

Acknowledgements

We thank the micro-fabrication centre of National Laboratory of Solid State Microstructures (NLSSM) for technical support. This work is jointly supported by the National Key Research and Development Program of China (no. 2017YFA0205700), National Natural Science Foundation of China (nos 52002168, 51925204, 11874211 and 61735008) and Natural Science Foundation of Jiangsu Province (no. BK20190311). W.L. and S.F. acknowledge the support of US Department of Energy grant no. DE-FG-07ER46426.

Author contributions

B.Z. and J.Z. conceived and designed the project. D.L., X.L., J.L. and B.L. performed the material preparation and characterization. D.L., X.L. and W.L. contributed to the optical and thermal measurement and analysis. W.L., Z. Lin and Z. Li performed the calculations. All authors contributed to the writing of the manuscript.

Competing interests

The authors declare no competing interests.

Additional information

Supplementary information is available for this paper at https://doi.org/10.1038/s41565-020-00800-4.

Correspondence and requests for materials should be addressed to B.Z. or J.Z.

Peer review information *Nature Nanotechnology* thanks the anonymous reviewers for their contribution to the peer review of this work.